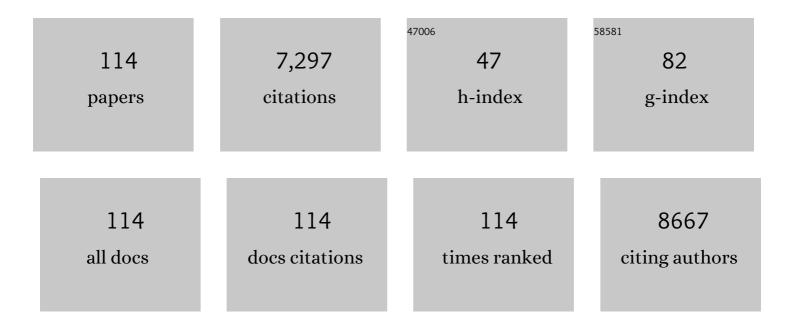
List of Publications by Year in descending order

Source: https://exaly.com/author-pdf/6259093/publications.pdf Version: 2024-02-01



#	Article	IF	CITATIONS
1	Interface engineering of MoS2@Fe(OH)3 nanoarray heterostucture: Electrodeposition of MoS2@Fe(OH)3 as N2 and H+ channels for artificial NH3 synthesis under mild conditions. Journal of Colloid and Interface Science, 2022, 606, 1374-1379.	9.4	15
2	Self-powered photoelectrochemical aptasensor based on MIL-68(In) derived In2O3 hollow nanotubes and Ag doped ZnIn2S4 quantum dots for oxytetracycline detection. Talanta, 2022, 240, 123153.	5.5	9
3	Z-scheme bismuth-rich bismuth oxide iodide/bismuth oxide bromide hybrids with novel spatial structure: Efficient photocatalytic degradation of phenolic contaminants accelerated by in situ generated redox mediators. Journal of Colloid and Interface Science, 2022, 614, 233-246.	9.4	28
4	A sensitive biosensor of CdS sensitized BiVO4/GaON composite for the photoelectrochemical immunoassay of procalcitonin. Sensors and Actuators B: Chemical, 2021, 329, 129244.	7.8	13
5	High-performance ammonia fixation electrocatalyzed by ReS ₂ nanosheet array. New Journal of Chemistry, 2021, 45, 11457-11460.	2.8	2
6	Molecular imprinted photoelectrochemical sensor for bisphenol A supported by flower-like AgBiS2/In2S3 matrix. Sensors and Actuators B: Chemical, 2021, 330, 129387.	7.8	15
7	Fabrication of MOF-derived tubular In2O3@SnIn4S8 hybrid: Heterojunction formation and promoted photocatalytic reduction of Cr(VI) under visible light. Journal of Colloid and Interface Science, 2021, 596, 278-287.	9.4	34
8	[Ru(bpy) ₃] ²⁺ @Ce-UiO-66/Mn:Bi ₂ S ₃ Heterojunction and Its Exceptional Photoelectrochemical Aptasensing Properties for Ofloxacin Detection. ACS Applied Bio Materials, 2021, 4, 7186-7194.	4.6	13
9	Photoelectrochemical competitive immunosensor for 17β-estradiol detection based on ZnIn2S4@NH2-MIL-125(Ti) amplified by PDA NS/Mn:ZnCdS. Biosensors and Bioelectronics, 2020, 148, 111739.	10.1	39
10	Adsorption and photocatalytic reduction of aqueous Cr(VI) by Fe3O4-ZnAl-layered double hydroxide/TiO2 composites. Journal of Colloid and Interface Science, 2020, 562, 493-501.	9.4	44
11	Enzyme-Free Colorimetric Immunoassay for Protein Biomarker Enabled by Loading and Disassembly Behaviors of Polydopamine Nanoparticles. ACS Applied Bio Materials, 2020, 3, 8841-8848.	4.6	14
12	Anchoring Au(111) on a Bismuth Sulfide Nanorod: Boosting the Artificial Electrocatalytic Nitrogen Reduction Reaction under Ambient Conditions. ACS Applied Materials & Interfaces, 2020, 12, 55838-55843.	8.0	35
13	Fabrication of N-GQDs and AgBiS2 dual-sensitized ZIFs-derived hollow ZnxCo3xO4 dodecahedron for sensitive photoelectrochemical aptasensing of ampicillin. Sensors and Actuators B: Chemical, 2020, 320, 128387.	7.8	23
14	Aerobic biodegradation of p-nitrophenol in a nitrifying sludge bioreactor: System performance, sludge property and microbial community shift. Journal of Environmental Management, 2020, 265, 110542.	7.8	20
15	Novel electrochemical immunosensor for sensitive monitoring of cardiac troponin I using antigen–response cargo released from mesoporous Fe3O4. Biosensors and Bioelectronics, 2019, 143, 111608.	10.1	32
16	A label-free photoelectrochemical aptasensing platform base on plasmon Au coupling with MOF-derived In2O3@g-C3N4 nanoarchitectures for tetracycline detection. Sensors and Actuators B: Chemical, 2019, 298, 126817.	7.8	71
17	A ternary quenching electrochemiluminescence insulin immunosensor based on Mn2+ released from MnO2@Carbon core-shell nanospheres with ascorbic acid quenching AuPdPt–MoS2@TiO2 enhanced luminol. Biosensors and Bioelectronics, 2019, 142, 111551.	10.1	36
18	Synergistic adsorption and photocatalytic reduction of Cr(VI) using Zn-Al-layered double hydroxide and TiO2 composites. Applied Surface Science, 2019, 492, 487-496.	6.1	35

#	Article	IF	CITATIONS
19	MnCO ₃ as a New Electrochemiluminescence Emitter for Ultrasensitive Bioanalysis of β-Amyloid _{1–42} Oligomers Based on Site-Directed Immobilization of Antibody. ACS Applied Materials & Interfaces, 2019, 11, 7157-7163.	8.0	54
20	A MoS ₂ nanosheet–reduced graphene oxide hybrid: an efficient electrocatalyst for electrocatalytic N ₂ reduction to NH ₃ under ambient conditions. Journal of Materials Chemistry A, 2019, 7, 2524-2528.	10.3	145
21	Efficient removal of graphene oxide by Fe3O4/MgAl-layered double hydroxide and oxide from aqueous solution. Journal of Molecular Liquids, 2019, 284, 300-306.	4.9	10
22	Cobalt-based metal-organic frameworks as co-reaction accelerator for enhancing electrochemiluminescence behavior of N-(aminobutyl)-N-(ethylisoluminol) and ultrasensitive immunosensing of amyloid-β protein. Sensors and Actuators B: Chemical, 2019, 291, 319-328.	7.8	42
23	Adsorption of phosphate from aqueous solution by vegetable biochar/layered double oxides: Fast removal and mechanistic studies. Bioresource Technology, 2019, 284, 65-71.	9.6	128
24	A prostate-specific antigen electrochemical immunosensor based on Pd NPs functionalized electroactive Co-MOF signal amplification strategy. Biosensors and Bioelectronics, 2019, 132, 97-104.	10.1	93
25	Quench-type electrochemiluminescence immunosensor for detection of amyloid β-protein based on resonance energy transfer from luminol@SnS2-Pd to Cu doped WO3 nanoparticles. Biosensors and Bioelectronics, 2019, 133, 192-198.	10.1	54
26	Fabrication of hierarchical MIL-68(In)-NH2/MWCNT/CdS composites for constructing label-free photoelectrochemical tetracycline aptasensor platform. Biosensors and Bioelectronics, 2019, 135, 88-94.	10.1	48
27	Magnetic electrode-based electrochemical immunosensor using amorphous bimetallic sulfides of CoSnSx as signal amplifier for the NT pro BNP detection. Biosensors and Bioelectronics, 2019, 131, 250-256.	10.1	17
28	CuS as co-reaction accelerator in PTCA-K2S2O8 system for enhancing electrochemiluminescence behavior of PTCA and its application in detection of amyloid-β protein. Biosensors and Bioelectronics, 2019, 126, 222-229.	10.1	68
29	Rod-like Bi4O7 decorated Bi2O2CO3 plates: Facile synthesis, promoted charge separation, and highly efficient photocatalytic degradation of organic contaminants. Journal of Colloid and Interface Science, 2018, 514, 240-249.	9.4	41
30	In situ Formed Co(TCNQ) ₂ Metalâ€Organic Framework Array as a Highâ€Efficiency Catalyst for Oxygen Evolution Reactions. Chemistry - A European Journal, 2018, 24, 2075-2079.	3.3	29
31	EDTA modified β-cyclodextrin/chitosan for rapid removal of Pb(II) and acid red from aqueous solution. Journal of Colloid and Interface Science, 2018, 523, 56-64.	9.4	111
32	Qualitative and quantitative spectrometric evaluation of soluble microbial products formation in aerobic granular sludge system treating nitrate wastewater. Bioprocess and Biosystems Engineering, 2018, 41, 841-850.	3.4	4
33	Label-free photoelectrochemical immunosensor for carcinoembryonic antigen detection based on g-C3N4 nanosheets hybridized with Zn0.1Cd0.9S nanocrystals. Sensors and Actuators B: Chemical, 2018, 256, 812-819.	7.8	41
34	Self-supported CoMoS4 nanosheet array as an efficient catalyst for hydrogen evolution reaction at neutral pH. Nano Research, 2018, 11, 2024-2033.	10.4	147
35	Ultrasensitive photoelectrochemical immunosensor for insulin detection based on dual inhibition effect of CuS-SiO2 composite on CdS sensitized C-TiO2. Sensors and Actuators B: Chemical, 2018, 258, 1-9.	7.8	38
36	Novel electrochemiluminescent platform based on gold nanoparticles functionalized Ti doped BiOBr for ultrasensitive immunosensing of NT-proBNP. Sensors and Actuators B: Chemical, 2018, 277, 401-407.	7.8	10

#	Article	IF	CITATIONS
37	A competitive photoelectrochemical immunosensor for the detection of diethylstilbestrol based on an Au/UiO-66(NH2)/CdS matrix and a direct Z-scheme Melem/CdTe heterojunction as labels. Biosensors and Bioelectronics, 2018, 117, 575-582.	10.1	56
38	Room-temperature fabrication of bismuth oxybromide/oxyiodide photocatalyst and efficient degradation of phenolic pollutants under visible light. Journal of Hazardous Materials, 2018, 358, 20-32.	12.4	49
39	Porous Fe–N-codoped carbon microspheres: an efficient and durable electrocatalyst for oxygen reduction reaction. Inorganic Chemistry Frontiers, 2018, 5, 2211-2217.	6.0	8
40	Removal of Pb(II) and methylene blue from aqueous solution by magnetic hydroxyapatite-immobilized oxidized multi-walled carbon nanotubes. Journal of Colloid and Interface Science, 2017, 494, 380-388.	9.4	140
41	Facile synthesis of hierarchical ZnIn 2 S 4 /CdIn 2 S 4 microspheres with enhanced visible light driven photocatalytic activity. Applied Surface Science, 2017, 407, 328-336.	6.1	67
42	Production of soluble microbial products in aerobic granular sludge system under the stress of toxic 4-chlorophenol. Environmental Technology (United Kingdom), 2017, 38, 3192-3200.	2.2	8
43	Fabrication of a novel Z-scheme g-C 3 N 4 /Bi 4 O 7 heterojunction photocatalyst with enhanced visible light-driven activity toward organic pollutants. Journal of Colloid and Interface Science, 2017, 501, 123-132.	9.4	102
44	Facile fabrication of BiOI decorated NaNbO 3 cubes: A p–n junction photocatalyst with improved visible-light activity. Applied Surface Science, 2017, 416, 288-295.	6.1	45
45	Comparison of soluble microbial products released from activated sludge and aerobic granular sludge systems in the presence of toxic 2,4-dichlorophenol. Bioprocess and Biosystems Engineering, 2017, 40, 309-318.	3.4	9
46	Fabrication of novel g-C3N4 nanocrystals decorated Ag3PO4 hybrids: Enhanced charge separation and excellent visible-light driven photocatalytic activity. Journal of Hazardous Materials, 2017, 339, 9-21.	12.4	73
47	Increased electrocatalyzed performance through high content potassium doped graphene matrix and aptamer tri infinite amplification labels strategy: Highly sensitive for matrix metalloproteinases-2 detection. Biosensors and Bioelectronics, 2017, 94, 694-700.	10.1	101
48	Fabrication of heterostructured Bi2O2CO3/Bi2O4 photocatalyst and efficient photodegradation of organic contaminants under visible-light. Journal of Hazardous Materials, 2017, 333, 169-178.	12.4	94
49	Sulfur-Doped Graphene-Based Immunological Biosensing Platform for Multianalysis of Cancer Biomarkers. ACS Applied Materials & Interfaces, 2017, 9, 37637-37644.	8.0	144
50	Magnetic chitosan/anaerobic granular sludge composite: Synthesis, characterization and application in heavy metal ions removal. Journal of Colloid and Interface Science, 2017, 508, 405-414.	9.4	83
51	Rapid removal of Pb(II) from aqueous solution using branched polyethylenimine enhanced magnetic carboxymethyl chitosan optimized with response surface methodology. Scientific Reports, 2017, 7, 10264.	3.3	37
52	Fabrication of In2S3/Zn2GeO4 composite photocatalyst for degradation of acetaminophen under visible light. Journal of Colloid and Interface Science, 2017, 506, 197-206.	9.4	56
53	A sensitive electrochemiluminescence immunosensor based on Ru(bpy) 3 2+ in 3D CuNi oxalate as luminophores and graphene oxide–polyethylenimine as released Ru(bpy) 3 2+ initiator. Biosensors and Bioelectronics, 2017, 89, 1020-1025.	10.1	100
54	Ultrasensitive electrochemical aptasensor for the detection of thrombin based on dual signal amplification strategy of Au@GS and DNA-CoPd NPs conjugates. Biosensors and Bioelectronics, 2016, 80, 640-646.	10.1	57

#	Article	IF	CITATIONS
55	Sensitive Insulin Detection based on Electrogenerated Chemiluminescence Resonance Energy Transfer between Ru(bpy) ₃ ²⁺ and Au Nanoparticle-Doped β-Cyclodextrin-Pb (II) Metal–Organic Framework. ACS Applied Materials & Interfaces, 2016, 8, 10121-10127.	8.0	87
56	Responses of soluble microbial products and extracellular polymeric substances to the presence of toxic 2,6-dichlorophenol in aerobic granular sludge system. Journal of Environmental Management, 2016, 183, 594-600.	7.8	33
57	Fabrication of highly active Melem/Zn0.25Cd0.75S composites for the degradation of bisphenol A and methyl orange under visible light irradiation. Applied Surface Science, 2016, 387, 513-520.	6.1	8
58	Facile solvothermal synthesis of Fe3O4/bentonite for efficient removal of heavy metals from aqueous solution. Powder Technology, 2016, 301, 632-640.	4.2	90
59	Preparation of Au-polydopamine functionalized carbon encapsulated Fe3O4 magnetic nanocomposites and their application for ultrasensitive detection of carcino-embryonic antigen. Scientific Reports, 2016, 6, 21017.	3.3	15
60	Fabrication of magnetic water-soluble hyperbranched polyol functionalized graphene oxide for high-efficiency water remediation. Scientific Reports, 2016, 6, 28924.	3.3	41
61	Ru(bpy)32+/nanoporous silver-based electrochemiluminescence immunosensor for alpha fetoprotein enhanced by gold nanoparticles decorated black carbon intercalated reduced graphene oxide. Scientific Reports, 2016, 6, 20348.	3.3	13
62	Magnetic hydroxypropyl chitosan functionalized graphene oxide as adsorbent for the removal of lead ions from aqueous solution. Desalination and Water Treatment, 2016, 57, 3975-3984.	1.0	24
63	Sandwich-type electrochemical immunosensor for the detection of AFP based on Pd octahedral and APTES-M-CeO2-GS as signal labels. Biosensors and Bioelectronics, 2016, 79, 482-487.	10.1	65
64	Ultrasensitive electrochemical immunosensor for SCCA detection based on ternary Pt/PdCu nanocube anchored on three-dimensional graphene framework for signal amplification. Biosensors and Bioelectronics, 2016, 79, 71-78.	10.1	73
65	Electrochemiluminescent immunosensing of prostate-specific antigen based on silver nanoparticles-doped Pb (II) metal-organic framework. Biosensors and Bioelectronics, 2016, 79, 379-385.	10.1	97
66	Cubic Cu 2 O nanoframes with a unique edge-truncated structure and a good electrocatalytic activity for immunosensor application. Biosensors and Bioelectronics, 2016, 78, 167-173.	10.1	39
67	Anaerobic granular sludge-derived activated carbon: preparation, characterization and superior dye adsorption capacity. Desalination and Water Treatment, 2016, 57, 18016-18027.	1.0	2
68	Novel gold nanocluster electrochemiluminescence immunosensors based on nanoporous NiGd–Ni2O3–Gd2O3 alloys. Biosensors and Bioelectronics, 2016, 75, 142-147.	10.1	19
69	Facile synthesized highly active BiOI/Zn ₂ GeO ₄ composites for the elimination of endocrine disrupter BPA under visible light irradiation. New Journal of Chemistry, 2015, 39, 3964-3972.	2.8	26
70	A biomimetic mussel-inspired photoelectrochemical biosensing chip for the sensitive detection of CD146. Analyst, The, 2015, 140, 5019-5022.	3.5	16
71	Synthesis of PtPb hollow nanoparticles and their application in an electrochemical immunosensor as signal tags for detection of dimethyl phthalate. RSC Advances, 2015, 5, 57346-57353.	3.6	6
72	Ultrasensitive sandwich-type electrochemical immunosensor based on a novel signal amplification strategy using highly loaded palladium nanoparticles/carbon decorated magnetic microspheres as signal labels. Biosensors and Bioelectronics, 2015, 68, 757-762.	10.1	35

#	Article	IF	CITATIONS
73	A novel magnetic polysaccharide–graphene oxide composite for removal of cationic dyes from aqueous solution. New Journal of Chemistry, 2015, 39, 2908-2916.	2.8	29
74	A simple label-free photoelectrochemical immunosensor for highly sensitive detection of aflatoxin B ₁ based on CdS–Fe ₃ O ₄ magnetic nanocomposites. RSC Advances, 2015, 5, 19581-19586.	3.6	27
75	Aerobic granular sludge-derived activated carbon: mineral acid modification and superior dye adsorption capacity. RSC Advances, 2015, 5, 25279-25286.	3.6	31
76	Efficient photocatalytic degradation of bisphenol A and dye pollutants over BiOI/Zn ₂ SnO ₄ heterojunction photocatalyst. RSC Advances, 2015, 5, 10688-10696.	3.6	30
77	Fabrication of a heterostructured Ag/AgCl/Bi ₂ MoO ₆ plasmonic photocatalyst with efficient visible light activity towards dyes. RSC Advances, 2015, 5, 17245-17252.	3.6	31
78	Fabrication of hierarchical BiOI/Bi2MoO6 heterojunction for degradation of bisphenol A and dye under visible light irradiation. Journal of Alloys and Compounds, 2015, 634, 223-231.	5.5	100
79	Electrochemiluminescence modified electrodes based on RuSi@Ru(bpy)32+ loaded with gold functioned nanoporous CO/Co3O4 for detection of mycotoxin deoxynivalenol. Biosensors and Bioelectronics, 2015, 70, 28-33.	10.1	29
80	EDTA functionalized magnetic graphene oxide for removal of Pb(II), Hg(II) and Cu(II) in water treatment: Adsorption mechanism and separation property. Chemical Engineering Journal, 2015, 281, 1-10.	12.7	576
81	An electrochemiluminescent immunosensor based on CdS–Fe ₃ O ₄ nanocomposite electrodes for the detection of Ochratoxin A. New Journal of Chemistry, 2015, 39, 4259-4264.	2.8	10
82	An ultrasensitive electrochemical immunosensor for CEA using MWCNT-NH ₂ supported PdPt nanocages as labels for signal amplification. Journal of Materials Chemistry B, 2015, 3, 2006-2011.	5.8	60
83	Kinetic, isotherm and thermodynamic investigations of phosphate adsorption onto core–shell Fe3O4@LDHs composites with easy magnetic separation assistance. Journal of Colloid and Interface Science, 2015, 448, 508-516.	9.4	246
84	Eco-friendly synthesis of electrochemiluminescent nitrogen-doped carbon quantum dots from diethylene triamine pentacetate and their application for protein detection. Carbon, 2015, 91, 144-152.	10.3	75
85	An ultrasensitive electrochemical immunosensor for the detection of CD146 based on TiO ₂ colloidal sphere laden Au/Pd nanoparticles. Analyst, The, 2015, 140, 3557-3564.	3.5	13
86	The removal of lead ions from aqueous solution by using magnetic hydroxypropyl chitosan/oxidized multiwalled carbon nanotubes composites. Journal of Colloid and Interface Science, 2015, 451, 7-14.	9.4	118
87	A label-free electrochemical immunosensor with a novel signal production and amplification strategy based on three-dimensional pine-like Au–Cu nanodendrites. RSC Advances, 2015, 5, 31262-31269.	3.6	9
88	An ultrasensitive electrochemical immunosensor for determination of estradiol using coralloid Cu ₂ S nanostructures as labels. RSC Advances, 2015, 5, 6512-6517.	3.6	19
89	A novel electrochemiluminescent immunosensor based on the quenching effect of aminated graphene on nitrogen-doped carbon quantum dots. Analytica Chimica Acta, 2015, 889, 82-89.	5.4	62
90	Corallite-like Magnetic Fe ₃ O ₄ @MnO ₂ @Pt Nanocomposites as Multiple Signal Amplifiers for the Detection of Carcinoembryonic Antigen. ACS Applied Materials & Interfaces, 2015, 7, 18786-18793.	8.0	63

#	Article	IF	CITATIONS
91	A novel electrochemical immunosensor using β-cyclodextrins functionalized silver supported adamantine-modified glucose oxidase as labels for ultrasensitive detection of alpha-fetoprotein. Analytica Chimica Acta, 2015, 893, 49-56.	5.4	31
92	Construction of dentate bonded TiO ₂ –CdSe heterostructures with enhanced photoelectrochemical properties: versatile labels toward photoelectrochemical and electrochemical sensing. Dalton Transactions, 2015, 44, 773-781.	3.3	38
93	Facile fabrication of heterostructured g-C ₃ N ₄ /Bi ₂ MoO ₆ microspheres with highly efficient activity under visible light irradiation. Dalton Transactions, 2015, 44, 1601-1611.	3.3	106
94	A competitive photoelectrochemical assay for estradiol based on in situ generated CdS-enhanced TiO2. Biosensors and Bioelectronics, 2015, 66, 596-602.	10.1	35
95	Electrochemiluminescent Immune-Modified Electrodes Based on Ag ₂ Se@CdSe Nanoneedles Loaded with Polypyrrole Intercalated Graphene for Detection of CA72-4. ACS Applied Materials & Interfaces, 2015, 7, 867-872.	8.0	34
96	Removal of mercury and methylene blue from aqueous solution by xanthate functionalized magnetic graphene oxide: Sorption kinetic and uptake mechanism. Journal of Colloid and Interface Science, 2015, 439, 112-120.	9.4	173
97	Aerobic granules formation and simultaneous nitrogen and phosphorus removal treating high strength ammonia wastewater in sequencing batch reactor. Bioresource Technology, 2014, 171, 211-216.	9.6	79
98	Adsorption of Pb(II) and Hg(II) from aqueous solution using magnetic CoFe2O4-reduced graphene oxide. Journal of Molecular Liquids, 2014, 191, 177-182.	4.9	215
99	Copper-doped titanium dioxide nanoparticles as dual-functional labels for fabrication of electrochemical immunosensors. Biosensors and Bioelectronics, 2014, 59, 335-341.	10.1	37
100	A label-free electrochemiluminescence immunosensor based on silver nanoparticle hybridized mesoporous carbon for the detection of Aflatoxin B1. Sensors and Actuators B: Chemical, 2014, 202, 53-59.	7.8	49
101	Novel visible-light driven g-C ₃ N ₄ /Zn _{0.25} Cd _{0.75} S composite photocatalyst for efficient degradation of dyes and reduction of Cr(<scp>vi</scp>) in water. RSC Advances, 2014, 4, 19980-19986.	3.6	21
102	Ultrasensitive dual amplification sandwich immunosensor for breast cancer susceptibility gene based on sheet materials. Analyst, The, 2014, 139, 3061-3068.	3.5	22
103	Mulberry-like gold nanospheres supported on graphene nanosheets: one-pot synthesis, characterization and photoelectrochemical property. New Journal of Chemistry, 2014, 38, 3166.	2.8	7
104	Ultrasensitive electrochemiluminescence immunosensor for detection of ochratoxin A based on gold nanoparticles-hybridized mesoporous carbon. Analytical Methods, 2014, 6, 5766-5770.	2.7	6
105	Facile fabrication of 3D flower-like heterostructured g-C ₃ N ₄ /SnS ₂ composite with efficient photocatalytic activity under visible light. RSC Advances, 2014, 4, 31019-31027.	3.6	71
106	Preparation and utilization of anaerobic granular sludge-based biochar for the adsorption of methylene blue from aqueous solutions. Journal of Molecular Liquids, 2014, 198, 334-340.	4.9	112
107	Nanosheet Au/Co3O4-based ultrasensitive nonenzymatic immunosensor for melanoma adhesion molecule antigen. Biosensors and Bioelectronics, 2014, 58, 345-350.	10.1	49
108	Metal ions-based immunosensor for simultaneous determination of estradiol and diethylstilbestrol. Biosensors and Bioelectronics, 2014, 52, 225-231.	10.1	66

#	Article	IF	CITATIONS
109	Synthesis of amino functionalized magnetic graphenes composite material and its application to remove Cr(VI), Pb(II), Hg(II), Cd(II) and Ni(II) from contaminated water. Journal of Hazardous Materials, 2014, 278, 211-220.	12.4	469
110	Enhanced aerobic granulation and nitrogen removal by the addition of zeolite powder in a sequencing batch reactor. Applied Microbiology and Biotechnology, 2013, 97, 9235-9243.	3.6	37
111	Removal of Metanil Yellow from water environment by amino functionalized graphenes (NH2-G) – Influence of surface chemistry of NH2-G. Applied Surface Science, 2013, 284, 862-869.	6.1	38
112	Label-free immunosensor for the detection of kanamycin using Ag@Fe3O4 nanoparticles and thionine mixed graphene sheet. Biosensors and Bioelectronics, 2013, 48, 224-229.	10.1	181
113	Highly efficient removal of heavy metal ions by amine-functionalized mesoporous Fe3O4 nanoparticles. Chemical Engineering Journal, 2012, 184, 132-140.	12.7	324
114	Adsorption of benzoic acid from aqueous solution by three kinds of modified bentonites. Journal of Colloid and Interface Science, 2011, 359, 499-504.	9.4	93